EXPERIMENTAL (FT-IR, FT-RAMAN) AND QUANTUM CHEMICAL STUDIES ON MOLECULAR STRUCTURE, SPECTROSCOPIC ANALYSIS, NLO, NBO AND REACTIVITY DESCRIPTORS OF 2-HYDROXY-6-METHYL-5-NITROPYRIDINE

N.Srinivasan[1],D.Mohan radheep[1] and K.Sambathkumar[2]

[1] R& Dcentre, Ponnaiyah Ramajayam Institute of science and Technology,Puducherry campus, Puducherry. India.

[2]P.G.&Research Department of Physics, (Computational and Theoretical Divisions), A.A.Govt.Arts College, Villupuram,India.

Abstract— The infrared and Raman spectra of 2-hydroxy-6-methyl- 5-nitropyridine [2,6,5-HMNP] were reported and compared with the theoretical results calculating at B3LYP/6-311+G(d,p) level. Both wave numbers and intensities obtained from the experimental and theoretical spectra were in good agreement. A complete spectral assignment was made with the aid of potential energy distribution (PED) based on the scaled quantum mechanical (SQM) force field method. Additionally, The HOMO-LUMO energy, Molecular electrostatic potential (MEP), natural bond orbitals (NBO) and non-linear optical (NLO) properties of the title molecule were studied theoretically on the same basis set.

Keywords:2,6,5-HMNP, HOMO- LUMO, NBO, MEP.

I.INTRODUCTION

The spectroscopic study of N-hetrocyclic molecules including substituted pyridines, pyrimidines have become quite interesting as they are the constituents of DNA and RNA and hence, play a central role in the structure and properties of the nucleic acids. The pyridine ring system is also very important as a structural unit in the natural products and compounds of pharmaceutical interest [1]. The spectroscopic study of the these compounds has been motivated for its use to understand the specific biological process and in the analysis of relatively complex system [2-5]. In pyridine system, a large amount of intermolecular association is possible because of its greater polarity. The nitrogen atom is located in sp^2-hybridized orbital, which is perpendicular to π-systems of the ring. A consequence of this structural feature is that the lone pair of electron and nitrogen atom is not associated with the ring and is available for pronotation. The basicity becomes more pronounced if electron-donating groups are present on the ring at second and sixth position, because they alter the electron availability on the nitrogen atom by resonance. The infrared spectroscopic investigation, however, formed part of larger programme of work involving the examination of the vibrational spectra from 4000-400 cm^{-1} of pyridine and substituted pyridines containing two, three and four substituents [6-8]. The objective of this investigation is to identify the vibrational frequencies corresponding to each substituents whether they are stretching vibrations or associated bending vibrations. It was also studied that the vibrations are dependent on the total number of substituents and their position in the ring. Hence, the vibrational spectra of 2-hydroxy-6-methyl-5-nitropyridine [2,6,5-H MNP] have been studied.

II EXPERIMENTAL

The spec-pure grade sample of 2,6,5-HMNP was obtained from the Lascaster Chemical Company, UK and used as such for the spectral measurements. The room temperature Fourier transform infrared spectra of the title compound was measured in the region 4000-400 cm^{-1} at a resolution of ± 1 cm^{-1} using a BRUKER 1FS-66V FTIR spectrometer equipped with dual detection a cooled MCT detector for the Mid-IR region. KBr Pellet was used in the spectral measurements. Boxcar apodization was used for the 250 averaged interferograms collected for the sample and background. The FT-Raman spectrum of 2,6,5-HMNP was recorded on a BRUKER IFS-66V model interferometer equipped with an FRA-106 FT-Raman accessory in the 3500 -100 cm^{-1} Stokes region using the 1064 nm line of a Nd: YAG laser for excitation operating at 200mw power. The reported wave numbers are believed to be accurate with in ± 1 cm^{-1}.

III COMPUTATIONAL DETAILS

Quantum chemical density functional calculations were carried out for 2,6,5-HMNP with the 09 Window version of the GAUSSIAN suite program [9] using the Becke-3-Lee-Yang-Parr (B3LYP) functionals supplemented with the standard 6-311+G(d,p) basis set (referred to as DFT calculations). The normal grid (50, 194) was used for numerical integration. All the parameters were allowed to relax and all the calculations

converged to an optimized geometry which corresponds to a true energy minimum, as revealed by the lack of imaginary values in the wave number calculations. The Cartesian representation of the theoretical force constants have been computed at the fully optimized geometry by assuming the molecule belongs to Cs point group symmetry. The transformation of force field from Cartesian to internal local-symmetry coordinates, the scaling, the subsequent normal coordinate analysis calculation of total energy distribution (TED).

IV RESULTS AND DISCUSSION

4.1 Molecular geometry

The molecular structure of the said molecule is shown in Fig 1. The molecule under consideration would belongs to C_s point group symmetry. The molecule has 17 atoms and one can expect 45 (3N-6) normal vibrations which are distributed as 31 in-plane vibrations of A′ species and 14 out-of-plane vibrations of A″. All the vibrations are active in both FTIR and Raman apart from these vibrations. The global minimum energy obtained by the DFT structure optimization for 2,6,5-HMNP is calculated as -567.2759 Hartrees. The calculated optimized geometrical parameters obtained in this study is presented in Table .1. Detailed description of vibrational modes can be given by means of normal coordinate analysis (NCA). For this purpose, the full set of 57 standard internal coordinates (Containing 12 redundancies) were defined in Table .2. From these, a non-redundant set of local symmetry coordinates were constructed by suitable linear combination of internal coordinates following the recommendations of Fogarasi and Pulay [10] are summarized in Table 3. The theoretically calculated DFT force fields were transformed to this latter set of vibrational coordinates and used in all the subsequent calculations.

V VIBRATIONAL SPECTRA

The vibrational analysis of 2,6,5-HMNP are made the basis of the magnitude and relative intensity of the recorded spectra and in analogy with the assignment made by the earlier researchers on the similar type of molecules. The FTIR and FT-Raman spectra of 2,6,5 HMNP is shown in Fig.2 and 3, respectively. The detailed vibrational assignments of fundamental modes of 2,6,5-HMNP along with the observed and calculated frequencies and normal mode descriptions (characterized by TED) are reported in Table 4.

C-H Vibrations

The two hydrogen atoms left around the ring in 2,6,5- HMNP give rise to two C-H strectching, two C-H in-plane bending and two C-H out-of-plane bending vibrations. The hetroatomic structure shows the presence of C-H stretching vibrations in the region 3100-3000 cm^{-1}, which is the characteristic region for ready identification of C-H stretching vibrations [11], in this region, the bands are not affected appreciably by the nature of substitutions . Hence, the bands at 3002 cm^{-1} in IR and 3084 cm^{-1} in Raman spectrum are assigned to C-H stretching vibrations in the title compound.

CH_3 Vibrations

For the assignments of CH_3 group frequencies, nine fundamental vibrations can be associated to each CH_3 group. Three stretching, three bending, two rocking modes and single torsional mode describes the motion of the methyl group. The CH_3 symmetric stretch, frequency is established at 2912 cm^{-1} in IR and CH_3 in-plane stretch, frequencies are assigned at 2939 cm^{-1} in IR for the title compound [12]. These assignments are also supported by the literatures in addition to TED output. The two in-plane methyl hydrogen deformation modes are also well established. The symmetrical methyl bending mode at 1361 cm^{-1} in the Raman and out-of-plane bending mode at 1194 cm^{-1} in IR the band at 2729 cm^{-1} in infrared is attributed to CH_3 out-of-plane stretching mode in the A″ species. The methyl deformation modes mainly coupled with In-plane bending vibrations. The band obtained at 1032 cm^{-1} in IR and 998 cm^{-1} in Raman are assigned to CH_3 in-plane and out-of-plane rocking modes. The assignments of the band at 253 cm^{-1} in Raman is attributed to methyl twisting mode. The CH_3 in-plane bending mode obtained at 1430 cm^{-1}.

C-N vibrations

The C-N stretching frequencies in the side chain are a rather difficult task [12]. Since there are problems in identifying these frequencies from other vibrations. The C-N stretching usually lies in the region 1400-1200 cm^{-1}. In this study, the band observed at 1426 cm^{-1}, 1399 cm^{-1} and 1344 cm^{-1} in Raman are assigned to C-N stretching vibrations. The C-N bending vibration and deformation mode are assigned to 928 cm^{-1} in Raman and 470 cm^{-1} in IR The above results are in close agreement with literature values .

NO_2 vibrations

The nitro group substituted at the fifth position of the title compound gives rise to C-NO_2 stretching vibrations. In analogy with their study, strong FTIR band observed at 1503 cm^{-1} and a FTIR band at 1378 cm^{-1} are assigned to the asymmetric and symmetric stretching, respectively of the NO_2 group may be identified with a strong FT-IR band at 767 cm^{-1}. The NO_2 wagging and rocking modes are observed at 726 cm^{-1} in FTIR and 548 cm^{-1} in Raman spectra. The NO_2 twisting mode observed at 331 cm^{-1} in Raman. The assignments are in good agreements with those proposed in case of nitropyridine and in nitro benzenes [13].

C-C vibrations

The ring stretching vibrations are very much prominent in the spectrum of pyridine and its derivatives and are highly characteristic of aromatic ring itself. There are very wide fluctuations in intensity [13 in the absorption bands due to aromatic structures in the 1600-1500 cm^{-1} region. In this study the bands between 1599 cm^{-1} and 1623-1525 cm^{-1} in FTIR and FT- Raman spectra of title compound respectively. The higher percentage of total energy distribution (TED) obtained for this group encouraging and confirms the assignments proposed in this study for C-C stretching vibrations.

VI Natural bond orbital (NBO) analysis

NBO analysis has been carried out to explain the charge transfer or delocalization of charge due to the intramolecular interaction among bonds, and also provides a convenient basis for investigating charge transfer or conjugative interaction in molecular systems. Some

electron donor orbital, acceptor orbital and the interacting stabilization energy resulting from the second-order micro-disturbance theory are reported [14]. The larger the stabilization energy value, the more intensive is the interaction between electron donors and electron acceptors, i.e. the more donating tendency from electron donors to electron acceptors, the greater the extent of conjugation of the whole system. Delocalization of electron density between occupied Lewis-type (bond or lone pair) NBO orbitals and formally unoccupied (anti bond or Rydberg) non-Lewis NBO orbitals correspond to a stabilizing donor-acceptor interaction. The intramolecular interaction are formed by the overlap among σ(C–C), σ^*(C–C), σ(C–N), σ^*(C–N), π(C–C) and π*(C–C) orbitals. These interactions are predicted as increase in electron density (ED) in C–C anti-bonding orbital that weakens the respective bonds. These intramolecular charge transfer $\sigma \rightarrow \sigma^*$, $\pi \rightarrow \pi^*$ can induce large nonlinearity of the molecule. The strong intramolecular hyper conjugation interaction of the σ and π electrons of C–C, C–O and C–N to the anti C–C, C–H, C–O and C–N bond leads to stabilization of some part of the ring as evident from Table 5. NBO analysis was performed on the molecule at the B3LYP/6-311+G(d,p) level in order to elucidate the intramolecular, re-hybridization and delocalization of ED within the molecule. The σ system shows some contribution to the delocalization corresponds to the donor - acceptor interactions are ($C_2 – C_3$) → ($C_2 – O7$), ($C_3 – H_9$), ($N_{11} – C_5$), ($C_2 – O_7$) → (N_1 - C_6), ($C_6 – C_{14}$), (C_3 - H_9), bondings are shown in the Table 5.

VII HOMO-LUMO energy gap

Spatial distribution of molecular orbitals, especially those of highest occupied molecular orbital (HOMO) and lowest unoccupied molecular orbital (LUMO), are excellent indicators of electron transport in molecular systems [14]. The conjugated molecules are characterized by a small HOMO–LUMO separation, which is the result of a significant degree of ICT from the end-capping electron donor groups to the efficient electron-acceptor groups through conjugated path. The HOMO and LUMO orbitals are shown in Fig.4. Since the atomic π-orbitals point towards each other and have better overlap, an increase in π -character points the fact that sigma bonds are stronger as evidenced by NBO analysis. The positive phase is red and the negative one is green. It is clear from the Fig.4 that, while the HOMO localizes on the three bond regions (N1– C6, C5–N11, C3–H9, C6–C14,), a highly delocalized HOMO and LUMO indicates that the electrons can more readily move around the molecule and hence an improved ICT. On the other hand, the LUMO strongly localizes on the different bond regions (C2–N1, N1–C14, C4–H10, C2–O7) indicating the presence of favorable atomic centers within 2,6,5-HMNP for possible electrophilic attacks and its bioactivity. The chemical hardness and softness of molecule is a good indicator of the chemical stability of a molecule. From the HOMO–LUMO energy gap, one can find whether the molecule is hard or soft. The molecules having large energy gap are known as hard and molecules having a small energy gap are known as soft molecules. The HOMO-LUMO energies and other related properties of energy gap, ionization potential (I), the electron affinity (A), the absolute electronegativity (χ), the absolute hardness (η) and softness (S) for the 2,6,5-HMNP molecule have been calculated and values are given in Table 6. The molecular energy transfer of 2,6,5-HMNP compound is shown in Fig 4. HOMO and LUMO energy values for a molecule, electronegativity and chemical hardness can be calculated as follow:

$$\chi = \frac{I+A}{2} \text{ (Electronegativity)}$$

$$\mu = -\frac{(I+A)}{2} \text{ (Chemical potential)}$$

$$\eta = \frac{I-A}{2} \text{ (Chemical hardness)}$$

$s=1/2\eta$ (chemical softness), $\omega=\mu^2/2\eta$ (Electrophilicity index)

Where I and A are ionization potential and electron affinity; $I= -E_{HOMO}$ and $A= -E_{LUMO}$ respectively. The ground state (HOMO) energy is -6.6464 eV and the first exited state (LUMO) energy is -2.8011 eV. The ground state and first exited state energy gap of 2,6,5-HMNP is found to be 3.8453 eV. Hence, the energy gap of title compound 2,6,5-HMNP is low. The lowering of the HOMO-LUMO band gap is essentially a consequence of the large stabilization of the LUMO due to the strong electron-accepting ability of the electron-acceptor group.

Nonlinear optical properties

The hyperpolarizability (β_o), dipole moment (μ) and polarizability (α) were calculated using B3LYPmethod with 6-311++G(d,p) basis set on the basis of the finite-field approach [15]. The complete equations for calculating the magnitude of total static dipole moment (μ), the mean polarizability (α_{tot}), the anisotropy of the polarizability (α) and the mean hyperpolarizability (β), using the x, y, z components from Gaussian 09W output is as follows:

$$\mu = \mu_0 + \alpha_{ij}E_j + \beta_{ijk}E_jE_k + \ldots,$$

$$\alpha = \frac{\alpha_{xx} + \alpha_{yy} + \alpha_{zz}}{3}$$

$$\beta_{tot} = \sqrt{(\beta_{xxx}+\beta_{xyy}+\beta_{xzz})^2 + (\beta_{yyy}+\beta_{yzz}+\beta_{xxy})^2 + (\beta_{zzz}+\beta_{xxz}+\beta_{yyz})^2}$$

It is well known that the higher values of dipole moment, molecular polarizability, and hyperpolarizability are important for more active NLO properties. The maximum polarizablity and hyperpolarizability were calculated as 6.4759 x 10^{-23} esu and 3.1879 x10^{-30} esu given in Table 7. The calculated value of dipole moment (μ) was found to be 2.0006 Debye. The first order hyperpolarizability of 2,6,5-HMNP with B3LYP/6-311++G(d,p) basis set is 3.1879 x 10^{-30} five times greater than the value of urea (β_o = 0.6230 x 10^{-30} esu). From the computation, the high values of the hyperpolarizabilities of 2,6,5-HMNP are probably attributed to the charge transfer existing amid the benzene rings within the molecular skeleton. Urea is one of the ideal molecule utilized in investigating of the NLO properties of the compound. For this reason, urea was used often as a threshold value for comparative purpose only. These

results show that the title compound is good nonlinear optical (NLO) activity.

VIII MOLECULAR ELECTROSTATIC POTENTIAL (MEP)

In the present study, a 3D plot of molecular electrostatic potential (MEP) map of 2,6,5-HMNP is illustrated in Figs.5 -7. The MEP is a plot of electrostatic potential mapped onto the constant electron density surface. The MEP is a useful property to study reactivity given that an approaching electrophile will be attracted to negative regions (where the electron distribution effect is dominant). The majority area of the MEP shows negative region due to electrophilic attack indications with red color and positive region shows nucleophilic attack symptoms as blue color [16]. The importance of MEP lies in the fact that it simultaneously displays molecular size, shape as well as positive, negative and neutral electrostatic potential regions in terms of color grading (Figs.5-7) and is very useful in research of molecular structure with its physiochemical property relationship. The MEP maps allow us to visualize variably charged regions of a molecule in terms of color grading. Areas of low potential, red (negative MEP) are characterized by an abundance of electrons or greatest electron density. Areas of high potential, blue (positive MEP), are characterized by a relative absence of electrons. The MEP of the nitrogen and oxygen atom of 2,6,5-HMNP reveals interesting features. The regions are represented by red and yellow color appearing below and above the molecular plane of the O7 atom is the electron rich region. The different values of the electrostatic potential at the surface are represented by different colors. Potential increases in the order red < orange < yellow < green < blue. The color code of the map is in the range between -5.279 a.u. (deepest red) and 5.279 a.u. (deepest blue), where blue indicates the strongest attraction and red indicates the strongest repulsion in title molecule. As can be seen from the MEP map of the title molecule, while regions having the negative potential are over the nitrogen and oxygen atoms, the regions having the positive potential are over all hydrogen atoms.

IX Thermodynamic properties

Several calculated thermodynamic parameters, heat capacity $\left(C^{0}_{p,m}\right)$, entropy $\left(S^{0}_{m}\right)$ and enthalpy changes $\left(H^{0}_{m}\right)$ were computed at B3LYP/6-311++G(d,p) basis set by using perl script THERMO.PL [17] and are listed in Table 8. Thermodynamic functions are all values increasing with temperature ranging from 100 to 1000K due to the fact that the molecular vibrations intensities increase with temperature. The correlation equation among heat capacities, entropies, enthalpy changes with temperatures were fitted by quadratic formulas and the corresponding fitting factors (R^2) these thermodynamic properties are 0.9983, 0.9999 and 0.9992 respectively. The correlations plot of those shown in Fig 8. The thermodynamic correlation fitting equation is follows:

$$\left(C^{0}_{p,m}\right) = 12.0082 + 0.7136T - 3.0736 \times 10^{-4}T^2$$

$$\left(S^{0}_{m}\right) = 263.6898 + 0.7681T - 1.7904 \times 10^{-4}T^2$$

$$\left(H^{0}_{m}\right) = -7.7780 + 0.0890T + 2.1171 \times 10^{-4}T^2$$

All thermodynamic data provide useful information for further studies. They can be used to compute other thermodynamic energies according to relationships of thermodynamic functions and estimate directions of chemical reactions according to the second law of thermodynamics in thermo chemical field [32]. Notice: all thermodynamic calculations were done in gas phase and they are not valid in solution

X CONCLUSION

The SQM force field method based on DFT calculations at the B3LYP/6-311+G(d,p) level have been carried out to analyse the vibrational frequencies of 2,6,5-HMNP. The close agreement established between the experimental and scaled frequencies obtained using the large basis set 6-311+G(d,p)calculation is proved to be more reliable and accurate than the calculation of semi empirical methods (or) lower basis sets. This accuracy is desirable for resolving distributes in vibrational assignments and provides valuable insight for understanding the observed spectral features. The PED calculation regarding the normal modes of vibration provides a strong support for the frequency assignment. NBO analysis was made and it is indicating the intramolecular charge transfer between the bonding and antibonding orbitals. HOMO and LUMO energy gap explains the eventual charge transfer interactions taking place within the molecule. Furthermore, the thermodynamic, non-linear optical, first-order hyperpolarizabilities and total dipole moment properties of the compound have been calculated in order to get insight into the compound. The calculated first hyperpolarizability of the title compound is 3.1879×10^{-30} esu which is comparable with the reported values of similar derivatives and which is five times that of the standard NLO material urea.

REFERENCE

[1] K.Settu, K.Sambathkumar and A.Claude Elixir Vib. Spec. 91 0 (2016) 38381-38391.
[2] K.Sambathkumar1 and G.Ravichandran Elixir Comp. Chem. 91 (2016) 38077-38086.
[3] K.Sambathkumara & K.Settu Elixir Vib. Spec. 91 (2016) 38087-38098.
[4] D.Cecily Mary Glory, R.Madivanane & K.Sambathkumar Indian journal of pure and Applied Physics. Vol 55 2017(638-648).
[5] H.I. Abdulla,E.I. Bermani M.F Spectrochimica Acta, 57A (2001) 2659.
[6] B.S. Yadav, Singh Vir, Seema, S. Chand, Indian J. Phys. 71B (1997) 697
[7] Y.K. Agarwal, P.K. Verma, Indian J Phys, 75B (2003) 549.
[8] B.S. Yadav, Kumar Nitin, Kumar Manoj, M.K. Yadav. Indian J Phys, 80(1) (2006) 61.
[9] M. J. Frisch, G. W. Trucks, H. B. Schlegel, G. E. Scuseria, M. A. Robb, Gaussian 09, Revision E.01, Gaussian, Inc., Wallingford CT, 2009.
[10] P.Pulay, G.Fogarasi, X.Zhou, P.W. Taylor, Vib. Spectrosc. 1 (1990) 159.
[11] S.Manimarana, S.Jeyavijayan and K.Sambathkumar IJARMPS Vol.2,(2017) 2455-6998.
[12] D.Cecily Mary Glory, R.Madivanane, K.Sambathkumar, A.Claude and K.Settu Elixir Vib. Spec. 90 (2016) 37416-37430 37416.

[13] C.Sengamalai, M.Arivazhagan and K.Sampathkumar Elixir Comp. Chem. 56 (2013) 13291-13298.
[14] Kuppusamy Sambathkumar Spectrochimica Acta Part A: Molecular and Biomolecular Spectroscopy 147 (2015) 51–66.
[15] K. Sambathkumar , S. Jeyavijayan, M. Arivazhagan Spectrochimica Acta Part A: Molecular and Biomolecular Spectroscopy 147 (2015) 124–138.
[16] D. Cecily mary glory, K. Sambathkumar , R. Madivanane, N. Rajkamal,M. Venkatachalapathy J of Molecular Structure 1149 (2017) 112-127.
[17] K.Parivathini, S.Manimaran and K.Sambathkumar, K.Settu and A. Claude Elixir Computational Physics 102 (2017) 44325-44336.

Table 1
Optimized geometrical parameters of 2-hydroxy-6-methyl-5-nitropyrid ine obtained by B3LYP/6-311+G density functional calculations**

Bond length	Value (Å)
N_1 - C_2	1.39
C_2 -C_3	1.39
C_3 - C_4	1.39
C_4 - C_5	1.39
C_5 - C_6	1.39
C_6 - N_1	1.39
C_2 - O_7	1.43
O_7 -H_8	0.96
C_3 - H_9	1.09
C_4 - H_{10}	1.09
C_5 - N_{11}	1.47
N_{11} - O_{12}	1.36
N_{11} - O_{13}	1.36
C_6 - C_{14}	1.54
C_{14} - H_{15}	1.06
C_{14} - H_{16}	1.07
C_{14} - H_{17}	1.06
N_1 - C_2	1.39
C_2 -C_3	1.39
C_3 - C_4	1.39
C_4 - C_5	1.39
C_5 - C_6	1.39
C_6 - N_1	1.39
Bond angle	Value (º)
N_1 - C_2 - C_3	120.00
C_2 - C_3 - C_4	120.00
C_3 - C_4 - C_5	119.990
C_4 - C_5 - C_6	119.990
C_5 - C_6 - N_1	120.00
C_6 - N_1 - C_2	120.00
N_1 - C_2 - O_7	119.990
C_3 -C_2 - O_7	120.00
N_1 - C_2 - C_3	120.00

For numbering of atom refer Fig.1

Table 2.
Definition of internal coordinates of 2-hydroxy-6-methyl-5-nitropyridine

No.(i)	Symbol	Type	Definition
Stretching			
1	S_1	O-H	O_7- H_8
2-3	r_1	C-H	C_2-H_9, C_3-H_{10}
4-6	r_1	C-H (methyl)	C_{14}-H_{15}, C_{14} -H_{16}, C_{14}-H_{17}
7-9	Q_1	C-N	C_2-N_1, C_5-N_{11}, C_6-N_1
10-14		R_1	C-C
15-16	P_1	N-O	N_{11}-O_{12}, N_{11}-O_{13}
17	T_1	C-O	C_2-O_7
Bending			
18-23	β_1	Ring	N_1-C_2-C_3, C_2-C_3-C_4, C_3-C_4-C_5, C_4-C_5-C_6, C_5-C_6-N_1, C_6-N_1-C_2
24-27	α_1	C-C-H	C_2-C_3-H_9, C_4-C_3-H_9, C_3-C_4-H_{10}, C_5-C_4-H_{10}
28-30	α_1	C-C-H (methyl)	C_6-C_{14}-H_{15}, C_6-C_{14}-H_{16}, C_6-C_{14}-H_{17}
31-33			σ_1
34-35	π_1	C-C-N	C_6-C_5-N_{11}, C_6-C_5-N_{11}
36	θ_1	C-C-C	C_5-C_6-C_{14}
37	ρ_1	N-C-C	N_1-C_6-C_5
38	σ_1	O-N-O	O_{12}-N_{11}-O_{13}
39-40	φ_1	C-N-O	C_5-N_{11}-O_{12}, C_5-N_{11}-O_{13}
41	φ_1	N-C-O	N_1-C_2-O_7
42	γ_1	C-C-O	C_3-C_2-O_7

For numbering of atom refer Fig. 1.

Table 3 Definition of local symmetry coordinates and values of correspond ing scale factorshe refined 6-311+G(d,p) and 6-311++G(d,p)force fields for 2-hydroxy-6-methyl-5-nitropyridine

No	Symbol[a]	Definition[b]	Scale factors used in the calculation	
			6-311+G(d,p)	6-311++G(d,p)
1	OH	S_1	0.983	0.926
2-3	CH	r_2, r_3	0.983	0.917
4	CH_2 SS	$(r_4 + r_5 + r_6) / \sqrt{3}$	0.976	0.917
5	CH_2 ips	$(r_4 + r_5 + r_6) / \sqrt{3}$	0.976	0.917
6	CH_2 ops	$(r_5 - r_6) / \sqrt{2}$	0.976	1.023
7-9	CN	Q_5, Q_6, Q_8	0.983	0.966
10-14	CC	R_{10}, R_{11}, R_{12}, R_{13}, R_{14}	0.983	0.966
15	NO_2 ss	$(P_{15}+P_{16}) / \sqrt{2}$	0.920	0.966
16	NO_2 ips	$(P_{15}-P_{16}) / \sqrt{2}$	0.920	0.966
17	CO	T_{17}	0.983	0.966
18	R trigd	$(\beta_{18}-\beta_{19}+\beta_{20}-\beta_{21}+\beta_{22}-\beta_{23}) / \sqrt{6}$	0.967	0.966
19	R symd	$(-\beta_{18}-\beta_{19}+2\beta_{20}-\beta_{21}-\beta_{22}+2\beta_{23}) / \sqrt{12}$	0.967	0.976
20	R asymd	$(\beta_{18}-\beta_{19}+\beta_{21}-\beta_{22}) / 2$	0.967	0.958
21-22	b CH	$(\alpha_{24}-\alpha_{25}) / \sqrt{2}$, $(\alpha_{26}-\alpha_{27}) / \sqrt{2}$	0.982	0.904
23	CH_2 sb	$(-\alpha_{24}-\alpha_{25}-\alpha_{26}+\delta_{21}+\delta_{22}+\delta_{23}) / \sqrt{6}$	0.978	0.904
24	CH_2 ipb	$(-\delta_{21}-\delta_{22}-2\delta_{23}) / \sqrt{6}$	0.978	0.904
25	CH_2 ipb	$(\delta_{21}-\delta_{22}) / \sqrt{2}$	0.978	0.959
26	CH_2 ipr	$(2\alpha_{25}-\alpha_{24}-\alpha_{26}) / \sqrt{6}$	0.978	0.987
27	CH_2 opr	$(\alpha_{24}-\alpha_{26}) / \sqrt{2}$	0.978	0.895
28	b CN	$(\pi_{24}-\pi_{25}) / \sqrt{2}$	0.982	0.895
29	b CC	$(\theta_{26}-\theta_{27}) / \sqrt{2}$	0.982	0.895
30	NO_2 sciss	$(2\varphi_{28}-\varphi_{29}-\varphi_{30}) / \sqrt{6}$	0.876	0.895
31	NO_2 Rock	$(\varphi_{29}-\varphi_{30}) / \sqrt{2}$	0.876	0.861
32	NO_2 twist	$(\varphi_{29}+\varphi_{30}) / \sqrt{2}$	0.876	0.895
33	bCO	$(\varphi_{31}-\gamma_{32}) / \sqrt{2}$	0.982	0.831
34	bOH	ψ_{32}	0.982	0.831

These symbols are used for description of normal modes by TED in Table 4.The internal coordinates used here are in Table 2.

Table 4
Assignment of fundamental vibrations of 1,5-dinitronaphthalene by normal mode analysis based calculations usingB3LYP/6-311+G force field**

Symm Species C_s	Observed fundamentals (cm^{-1})		TED (%) among types of coordinates	
			Unscaled	
	FTIR	Raman	B3LYP/6-311+G(d,p)	
A′	3415(w)	-	3420	νOH (99)
A′	-	3084(w)	3088	νCH(97)
A′	3002(vw)	-	3002	νCH(94)
A′	2939 (w)	-	2936	CH_3ips(90)
A′	2912(ms)	-	2910	CH_3ss(88)
A′	-	1623(s)	1627	νCC (87)
A′	1599 (w)	-	1594	νCC(89)
A′	-	1587(ms)	1587	νCC(85)
A′	-	1545(s)	1549	νCC(82)
A′	-	1525(ms)	1520	νCC(83)
A′	1503 (S)	-	1500	NO_2ass(84)
A′	1430(m)	-	1432	CH_3 ipb (81)
A′	-	1426(ms)	1425	νCN(80)
A′	-	1399(s)	1405	νCN(78)
A′	1378(m)		1375	NO_2ss(79)
A′	-	1361(m)	1365	CH_3sb(76)
A′	1347(s)	-	1350	νCO(74)
A′	-	1344(vs)	1344	νCN(73)
A′	1243(vs)	-	1252	bCH (72)
A′	-	1210(ms)	1205	bCH (71)
A′	-	1190(s)	1187	bOH (70)
A′	1127(vw)	-	1126	R trigd (71)
A′	1096(vs)	-	1097	R symd(72)
A′	-	1038(m)	1042	Rasymd (73)
A′	1032(s)		1024	CH_3 ipr(70)
A′		928(w)	924	bCN(69)
A′		799(w)	802	bCO(68)
A′	767(s)		767	NO_2 sciss (69)
A′	602(vw)	-	595	bCC(67)
A′		548(s)	552	NO_2rock(69)
A″	2729(vw)		2728	CH_3ops(65)
A″	1194(m)		1194	CH_3opb(63)
A″	-	998(ms)	995	CH_3opr(64)
A″	958(m)	-	954	ωCH (62)
A″	932(m)		930	ωCH(64)
A″	726(ms)	-	731	NO_2 wag(61)
A″		663(s)	661	tR trigd (60)
A″	639(vs)		642	tR symd(62)
A″	543(m)		542	tR asymd(61)
A″	470(w)		471	ωCN (58)
A″		460(s)	460	ωCC(59)
A″		414(m)	416	ωCO (57)
A″		358(s)	356	ωOH (59)
A″		331(w)	335	NO_2 twist (56)
A″		253(vw)	252	tCH_3 (54)
A′	3415(w)	-	3420	νOH (99)
A′	-	3084(w)	3088	νCH(97)
A′	3002(vw)	-	3002	νCH(94)
A′	2939 (w)	-	2936	CH_3ips(90)
A′	2912(ms)	-	2910	CH_3ss(88)
A′	-	1623(s)	1627	νCC (87)
A′	1599 (w)	-	1594	νCC(89)
A′	-	1587(ms)	1587	νCC(85)
A′	-	1545(s)	1549	νCC(82)
A′	-	1525(ms)	1520	νCC(83)
A′	1503 (S)	-	1500	NO_2ass(84)
A′	1430(m)	-	1432	CH_3 ipb (81)
A′	-	1426(ms)	1425	νCN(80)
A′	-	1399(s)	1405	νCN(78)
A′	1378(m)		1375	NO_2ss(79)

Abbreviations :ss-symmetric stretching; ass-antisymmetric stretching; b-bending; R-Ring; t-torsion; ω-out-of-plane bending; vs – very strong; s – strong; ms – medium strong; m – medium; w – weak; vw-very weak.

Table 5.Second order perturbation theory analysis of Fock matrix in NBO basis for [2,6,5-HMNP]

Donor(i)	Type	ED/e	Acceptor(i)	Type	ED/e	^{a}E(2) (kJ mol^{-1})	^{b}E(j)-E(i) (a.u.)	^{c}F(i,j) (a.u.)
N_1-C_4	σ	1.9660	C_7-O_7	σ*	0.0114	2.920	1.170	0.052
			C_7-O_{12}	π*	0.2879	3.840	0.690	0.049
N_1-H_{13}	σ	1.9836	C_2-H_{13}	σ*	0.0167	3.880	0.940	0.054
C_2-H_{13}	σ	1.9887	C_7-H_9	σ*	0.0125	2.260	1.310	0.049
C_2-H_9	π	1.9272	C_7-C_8	π*	0.1667	11.370	0.350	0.058
C_7-C_8	σ	1.9884	C_7-H_9	σ*	0.0125	1.480	1.190	0.038
			C_7-H_{13}	σ*	0.0114	1.620	1.190	0.039
C_7-C_8	π	1.9026	N_1-N_{11}	π*	0.2204	9.300	0.280	0.047
C_7-H_9	σ	1.9856	N_1-C_6	σ*	0.0072	1.480	1.120	0.036
			C_7-N_{11}	σ*	0.0218	2.860	0.880	0.045
C_6-N_{11}	σ	1.9728	N_1-C_4	σ*	0.0533	2.250	0.990	0.042
			N_1-H_{13}	σ*	0.0188	5.050	1.110	0.067
C_7-N_4	σ	1.9755	C_7-H_2	σ*	0.0188	2.450	1.140	0.047
			C_7-H_9	σ*	0.0125	2.980	1.180	0.053
C_6-H_{11}	σ	1.9834	C_7-N_1	σ*	0.0167	2.730	0.920	0.045
C_7-O_7	σ	1.9847	C_7-N_1	σ*	0.0218	2.120	1.080	0.043
C_7-C_{14}	π	1.9619	C_7-C_{14}	π*	0.1413	6.550	0.320	0.042
C_{10}-C_{14}	σ	1.9771	N_1-C_{14}	σ*	0.0963	3.960	0.940	0.056
			C_7-C_8	σ*	0.0814	2.270	1.240	0.047
C_7-H_9	σ	1.9553	C_4	LP (1)	1.2449	10.060	0.330	0.081
			C_7-C_4	σ*	0.0897	3.290	1.030	0.052
			C_7-C_8	σ*	0.0454	5.110	1.030	0.065
C_7-C_8	σ	1.9724	C_7-C_9	σ*	0.0454	10.270	1.320	0.104
			C_7-C_8	σ*	0.0953	6.410	1.360	0.084
C_7-C_9	σ	1.9787	C_{11}-C_4	σ*	0.0814	4.830	1.300	0.071
			C_7-H_9	σ*	0.0191	3.440	1.090	0.055
C_7-C_9	π	1.7818	C_8	LP (1)	52.0000	62.340	0.080	0.093
			C_8-C_{12}	π*	0.6283	20.920	0.230	0.070
C_7-C_8	σ	1.9401	C_7-H_{10}	σ*	0.0130	3.680	1.140	0.058
			C_7-H_9	σ*	0.0953	4.570	1.260	0.068
C_7-C_{14}	σ	1.9774	C_7-H_8	σ*	0.0134	4.270	1.110	0.062
C_7-C_8	σ	1.9830	C_7-C_4	σ*	0.0814	6.010	1.580	0.087
C_7-C_4	π	1.9078	C_8	LP (1)	1.2449	33.410	0.200	0.112
N_1	LP(1)	1.7152	N_1-H_{13}	π*	0.2204	17.080	0.360	0.071
			C_7-C_8	π*	0.1667	12.350	0.390	0.064
N_{11}	LP(1)	1.9021	N_1-C_4	σ*	0.0533	9.080	0.690	0.071
			C_7-C_8	σ*	0.0139	3.050	1.010	0.050
O_7	LP(1)	1.9784	C_7-C_8	σ*	0.0897	3.290	1.240	0.057
O_{12}	LP(2)	1.8829	N_1-C_6	σ*	0.0963	24.590	0.570	0.106

[a]$E^{(2)}$ means energy of hyper conjugative interaction (stabilization energy)
[b]Energy difference between donor and acceptor i and j NBO orbitals.
[c]F(i,j) is the Fock matrix element between i and j NBO orbitals

Table 6.
Calculated energy values of title compound by B3LYP/6-311++G(d,p) method.

Parameters	B3LYP/6-311++G(d,p)
[illegible]	[illegible]
[illegible]	[illegible]
[illegible]	[illegible]
[illegible]	[illegible]
[illegible]	[illegible]
[illegible]	[illegible]
[illegible]	[illegible]
[illegible]	[illegible]
[illegible]	[illegible]
[illegible]	[illegible]

Table 7.
The values of calculated dipole moment μ(D), polarizability (α_0), first order hyperpolarizability (βtot) components of 2-hydroxy-6-methyl-5-nitropyridine

Parameters	B3LYP/6-311++G(d,p)	Parameters	B3LYP/6-311++G(d,p)
μ_x	-1.9702	β_{xxx}	-159.3038
μ_y	0.3414	β_{xxy}	109.5664
μ_z	-0.0668	β_{xyy}	1.2405
μ(D)	2.0006	β_{yyy}	90.1054
α_{xx}	243.4682	β_{zxx}	-33.2486
α_{xy}	29.0513	β_{xyz}	117.7755
α_{yy}	118.1247	β_{zyy}	95.2725
α_{xz}	47.6330	β_{xzz}	42.0856
α_{yz}	-3.4598	β_{yzz}	25.148
α_{zz}	144.3268	β_{zzz}	206.6094
α_0 (e.s.u)	$2.4992x10^{-23}$	βtot (e.s.u)	$3.1879X10^{-30}$
Δα(e.s.u)	$6.4759 x10^{-23}$		

Table 8
Temperature dependence of thermodynamic properties of 2-hydroxy-6-methyl-5-nitropyridine at B3LYP /6-311++G(d,P)

T(K)	(J/ mol K)	(J/ mol K)	(kJ/ mol)
100	87.413	337.558	6.304
200	135.441	411.972	17.312
298.15	193.576	476.779	33.433
300	194.676	477.98	33.792
400	250.434	541.822	56.118
500	296.311	602.827	83.542
600	332.491	660.182	115.055
700	361.066	713.665	149.787
800	384.025	763.431	187.082
900	402.823	809.783	226.454
1000	418.455	853.058	267.541

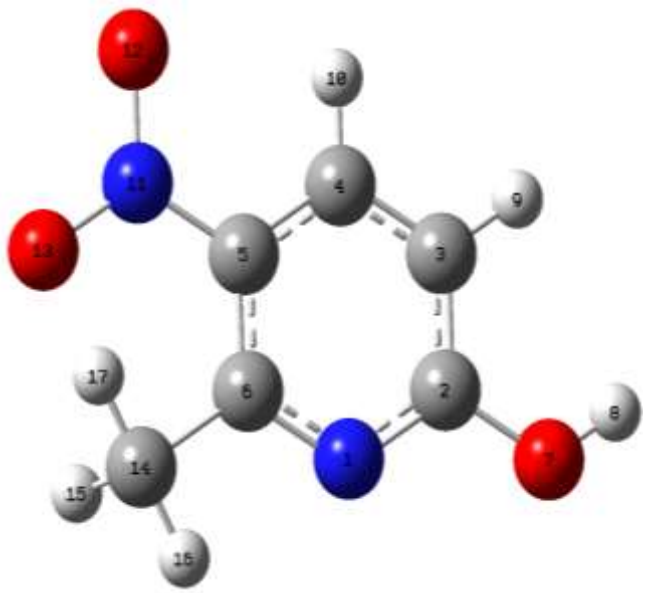

Fig.1 Molecular Structure of 2-hydroxy-6-methyl- 5-nitropyridine

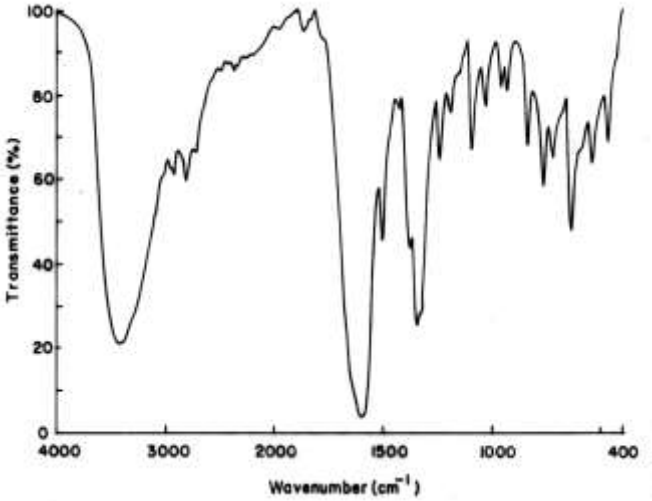

Fig. 2 Observed infrared spectra of 2-hydroxy-6-methyl- 5-nitropyridine

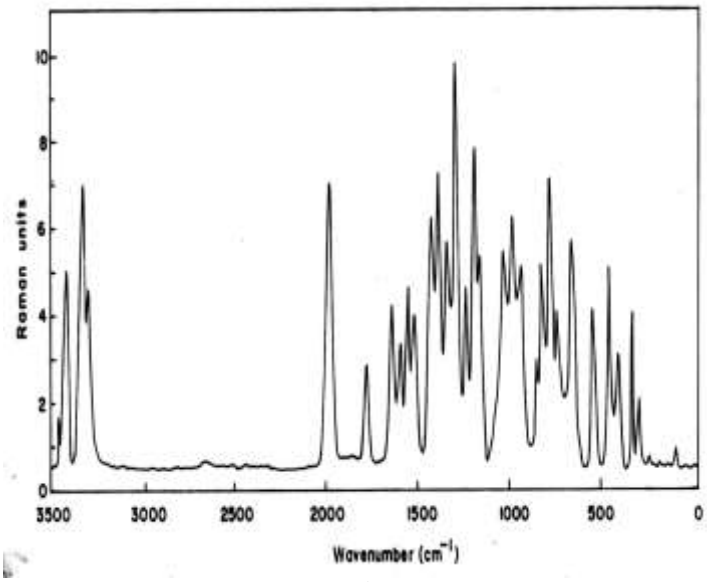

Fig. 3 Observed Raman spectra of 2-hydroxy-6-methyl- 5-nitropyridine

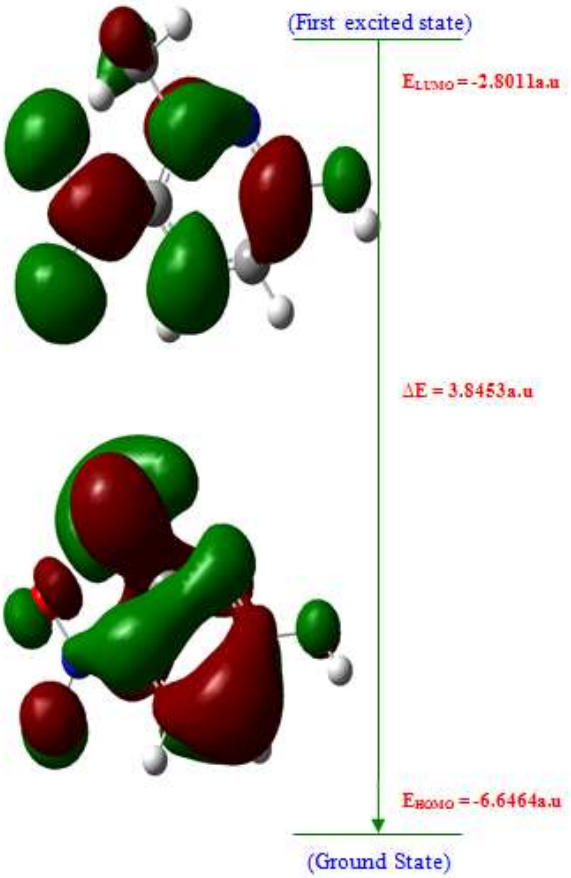

Fig. 4: HOMO-LUMO PLOT OF 2-HYDROXY-6-METHYL-5-NITROPYRIDINE

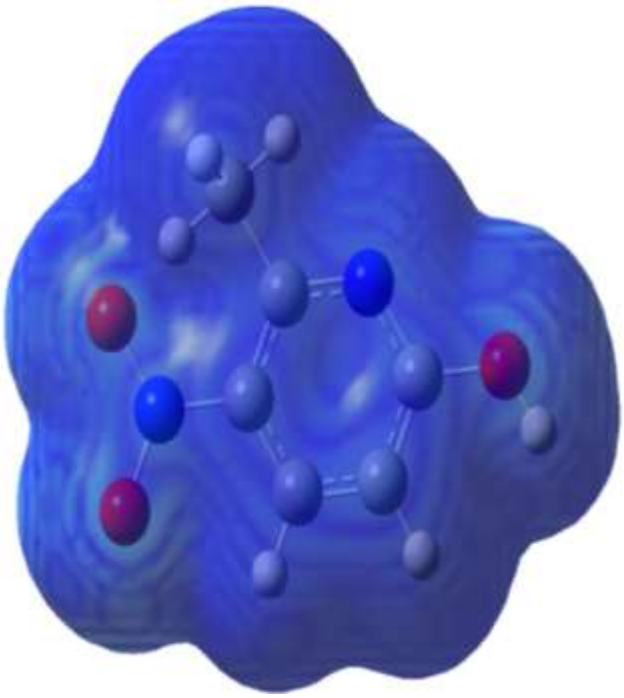

Fig 5.The total electron density surface of 2-hydroxy-6-methyl-5-nitropyridine.

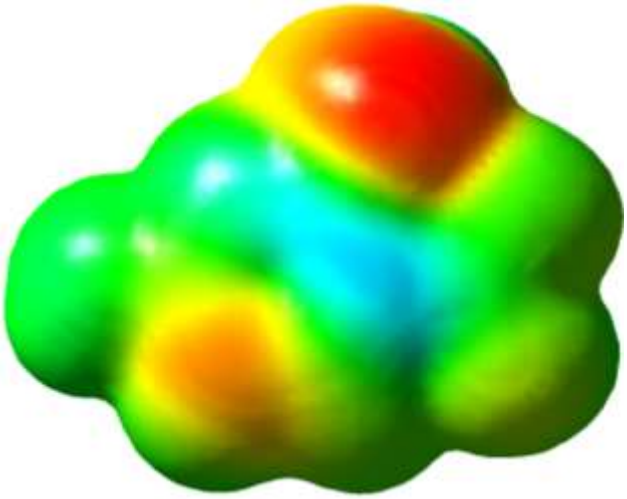

Fig 6.The molecular electrostatic potential surface of 2-hydroxy-6-methyl- 5-nitropyridine.

.

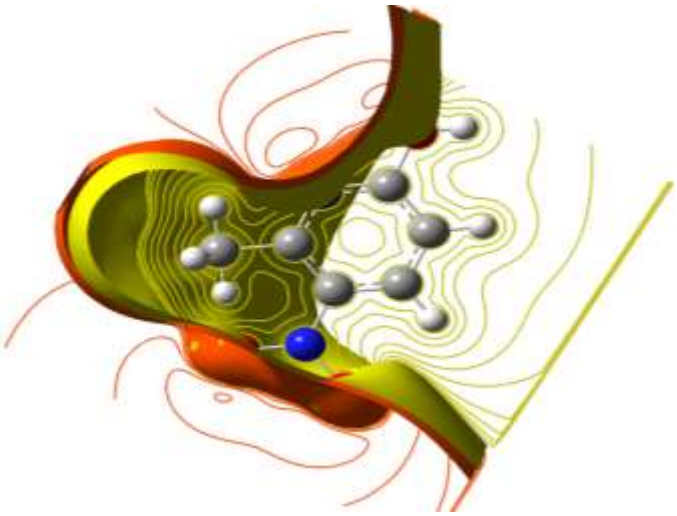

Fig 7.The contour map of the electrostatic potential surface of 2-hydroxy-6-methyl- 5-nitropyridine.

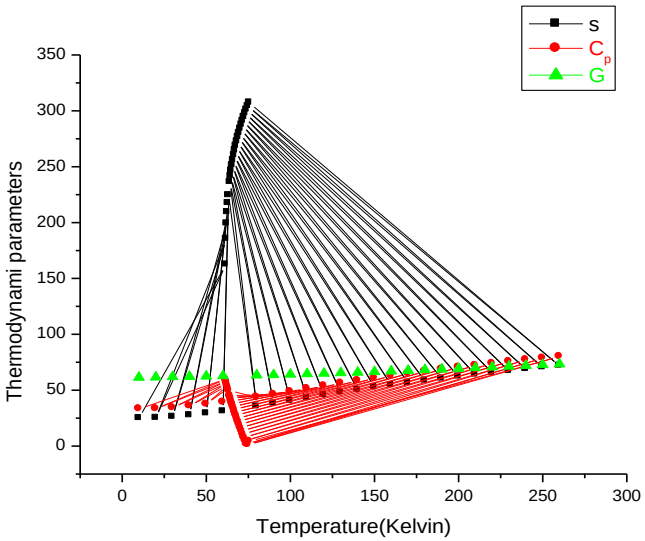

Fig 8. Correlation graphic of thermodynamic parameters and Temperature for entropy (S), heat capacity at constant pressure (Cp), Gibb's free energy(G) energy change of 2-hydroxy-6-methyl- 5-nitropyridine.